

## Synthesis and analysis of cellulose based layered double hydroxide nanocomposite adsorbent for arsenic removal from water

Tanveer Ahmed, Sajjad Haydar, Mehwish Anis\*

*Institute of Environmental Engineering and Research (IEER), University of Engineering and Technology (UET), 54890-G.T. Road Bahgpur Lahore, Pakistan, Tel. +92 429029248; emails: mehwish@uet.edu.pk (M. Anis), tanveerahmed@uet.edu.pk/tanveer.env58@gmail.com (T. Ahmed), sajjad@uet.edu.pk (S. Haydar)*

Received 2 September 2021; Accepted 8 February 2022

### ABSTRACT

Arsenic is a potential carcinogenic element and found in groundwater worldwide in concentration higher than the permissible limits for drinking. A low-cost solution for removal of arsenic from water was the objective of this study. A new adsorbent, that is, cotton linter cellulose (CLC) magnesium aluminum layered double hydroxide (LDH) bio-nanocomposite (CLC-Mg|Al LDH) was synthesized. The adsorbent and CLC were characterized using XRD and FTIR to identify difference in mixed phase of successful synthesis. Adsorbent was also characterized using BET, SEM, TEM and AFM techniques. XRD analysis showed that adsorbent was crystalline, TEM analysis showed that structure of adsorbent was sheet like having size range in nanometers. SEM analysis indicated that adsorbent had rough and porous surface while AFM results showed that adsorbent had good agglomeration of particles. After characterization optimization studies for various parameters was performed for arsenic removal. Optimum arsenic removal was achieved at pH, contact time, dose and temperature of 7, 25 min, 0.67 g/L and 25°C, respectively. Kinetic studies revealed adsorption followed pseudo-second-order model. Adsorption capacity of adsorbent was found to be 1.46 mg/g with 99.3% removal at 150 ppb initial arsenic concentration. Thermodynamic studies showed that adsorption process was spontaneous and exothermic. The cost of treatment came out to be USD 0.15/m<sup>3</sup> of treated water.

*Keywords:* Layered double hydroxide; Nanocomposite; Arsenic; Adsorption; Kinetics; Isotherm

### 1. Introduction

Presence of higher arsenic (As) in groundwater in concentrations above permissible limits of World Health Organization (WHO) is of concern in areas where groundwater is used for drinking purposes. WHO allowed maximum permissible limit of 10 ppb in drinking water [1]. Mostly occurring arsenic species in natural waters include H<sub>3</sub>AsO<sub>4</sub><sup>-</sup>, H<sub>2</sub>AsO<sub>4</sub><sup>2-</sup>, HAsO<sub>4</sub><sup>2-</sup>, and AsO<sub>4</sub><sup>3-</sup> (oxidation state V) and arsenite ions, H<sub>3</sub>AsO<sub>3</sub>, H<sub>2</sub>AsO<sub>3</sub><sup>-</sup> and HAsO<sub>3</sub><sup>2-</sup> (oxidation state III) [2]. As is toxic and carcinogenic [3] and is found as As(III) or As(V) oxidation states. Arsenic is responsible

for liver, kidney, lung and bladder cancer [4]. It also causes neurological changes, muscle weakness, skin pigmentation and loss of appetite [5]. Despite deleterious effects, people of many regions of the world are forced to drink arsenic contaminated water.

Many countries are facing the problem of high arsenic concentration in groundwater. These include China, Chili, Bangladesh, Mexico, USA and Pakistan. In different regions of India, arsenic concentration varies from 10 to 3,700 ppb. Therefore, arsenic related health issues were observed in 4.5% of the children and 10% of the adults in arsenic affected areas [6]. Similarly, many areas of Pakistan

\* Corresponding author.

including Tarbela, Chashma, Karachi, Lahore, Qasur, Vehari, Muzaffargarh, Bahawalpur and Rahimyar Khan have objectionable arsenic levels in groundwater [7,8]. Studies in Jehlum [9], Muzaffargarh [10], and Nagarparkar also revealed arsenic levels exceeding WHO guidelines (10 ppb) and lying in a range of 0–500,000 ppb [11,12].

Studies for removal of arsenic have been conducted using different methods viz. ion exchange, precipitation, electrochemical treatment, membrane separation and adsorption [13–17]. The above-mentioned technologies are not considered to be cost effective. In addition, these cannot meet the stringent standards [15,18]. Membrane system, affected by fouling, cannot be considered as cost-effective [19]. Ion exchange is affected by competing ions concentrations [20]. Electrochemical process was found to be pH dependent [21]. Chemical precipitation involves high operational costs and sludge handling issue [22]. Studies showed that among all technologies, adsorption is cost effective in removing specific contaminant [23].

Many adsorbents were employed for arsenic uptake from water and wastewater including activated carbon, crop residues, biomass, zeolite, iron, manganese, zirconium and many metal oxide nanoparticles [24–27]. Among these iron oxide based nanoparticles proved to be efficient [28]. With respect to arsenic, adsorption is regarded better than the other technologies. It is sludge free process, cost-effective and handled easily [29]. Thus, nanotechnology including nanoparticles and nanocomposite are the focus of recent research.

Many nanoparticles (as adsorbents) were designed, prepared and investigated for arsenic uptake. These include magnetite nanoparticles (MNP) [30], electrochemical cell of aluminum and iron [31], CuO-Fe<sub>3</sub>O<sub>4</sub> material using a combination of photo-oxidation of arsenic and subsequent adsorption, ZrO<sub>2</sub>-Fe<sub>3</sub>O<sub>4</sub> magnetic nanoparticles along with oxidation of arsenic(V) to arsenic(III) with light [30,32], Fe-Ce bimetal adsorbent [30], iron-cerium alkoxide (NH-ICA) [33] etc. Other nanoparticle include black carbon with modified surface, iron and aluminum hydroxides [34]. Nanoparticles have high regeneration capacity. However, focus is shifting to synthesize cost-effective bio-nanocomposite adsorbents using cellulose (CL) from different materials, that is, pectic, xanthan gum, aginate and k-carrageen etc.

CL, as renewable biomass, is present on earth in bulk quantities. It may be converted to CL-nanocomposite material for application in adsorption of toxic material, that is, arsenic. Examples of such materials include; CL-Au, CL-Ag, CL-CdS, CL-ZnO, CL-Fe<sub>2</sub>O<sub>3</sub>, CL-TiO<sub>2</sub>, CL-SiO<sub>2</sub>, CL-Mg-LDH nanocomposite, CL-Hydroxyapatite and CL-CaCO<sub>3</sub> [33,35]. Researchers are working to find CL based adsorbents with large surface areas, that is, layered doubled hydroxides (LDHs).

LDH, generally named as bi-dimensional anionic clays, have similar layered structure as brucite [36]. Main property of LDHs is that they show excess positive charge because of divalent ions are substituted with trivalent ions. Due to excess positive charge, various anions get attached in between the layers. LDHs are used for different purposes such as catalytic agents, antacids, inorganic and anion replacements etc. Different pollutants having organic or inorganic nature are treated with LDHs. Different organic

and inorganic nature substrates can be modified with LDHs as binding materials for synthesis of nanocomposite adsorbents [36,37].

Ion exchange, co-precipitation, and reformation of calcined LDH, in the presence of organic polymer are being used for synthesis of organic-LDH intercalations [37]. Different organic polymers, that is, pectic, xanthan gum, aginate, k-carrageen etc. had been used in synthesis of organic LDHs. Wide application of these synthesized organic LDHs has been witnessed including medical diagnosis, diet analysis and water quality check [38]. Many LDHs have been applied for removal of arsenic from water including Mg|Al-Chloride, Mg|Al-NO<sub>3</sub>, Mg|Al-CO<sub>3</sub>, Ca|Al-Chloride, Ca|Al-NO<sub>3</sub>, Fe|Mn-CO<sub>3</sub>, Fe|Mn-NO<sub>3</sub>, Zn|Fe LDH etc. showing good arsenic removal from water [39–41]. However, use of organic LDHs for the uptake of heavy metals and other contaminants needs to be investigated.

The main factors affecting arsenic removal from water are cost, applicability, removal efficiency, health effects of the material used, availability of materials used in adsorbent synthesis in bulk and recyclability [42]. Different variables affecting arsenic removal by an adsorbent are pH, temperature, turbidity, physical and chemical characteristics and flow of the water. Cost of treatment using adsorbents directly increase with increase in arsenic concentration in water sample.

Raw material available for adsorbent synthesis is also directly linked with application in the field. Adsorbent with higher cost has limited scope, especially for developing countries [43]. Materials with high surface areas and active sites with high desorption power, regeneration and recyclability are needed. Researchers could not provide the cost benefit analysis of many newly synthesized adsorbents. There is a need of finding feasibility, cost effectiveness and design procedures for proper application of new adsorbents [12].

In summary, numerous treatment methods were employed for arsenic removal. Among all only adsorption is considered most reliable and cost-effective. In this study a new bio-nanocomposite adsorbent was prepared using CLC. The purpose was to determine its capacity for the removal of arsenic from water. Its success may introduce a low-cost adsorbent for arsenic uptake in large scale water supplies.

## 2. Materials and methods

### 2.1. Chemical reagents

Laboratory grade magnesium chloride (MgCl<sub>2</sub>·6H<sub>2</sub>O), aluminum chloride (AlCl<sub>3</sub>·6H<sub>2</sub>O), cotton linter cellulose (CLC), sodium arsenite (NaAsO<sub>2</sub>), sodium arsenate (NaHAsO<sub>4</sub>), urea (NH<sub>2</sub>)<sub>2</sub>CO, sodium hydroxide (NaOH), ethyl alcohol (C<sub>2</sub>H<sub>5</sub>O) and sodium chloride (NaCl) were bought from Sigma-Aldrich.

### 2.2. Synthesis of adsorbent

Adsorbent was synthesized using coprecipitation method. The schematic diagram of adsorbent synthesis procedure is given in Fig. 1. For this purpose, a solution of NaOH, urea and H<sub>2</sub>O with mass ratios of 7, 12 and 81 g was prepared. This solution was precooled to –12°C to dissolve

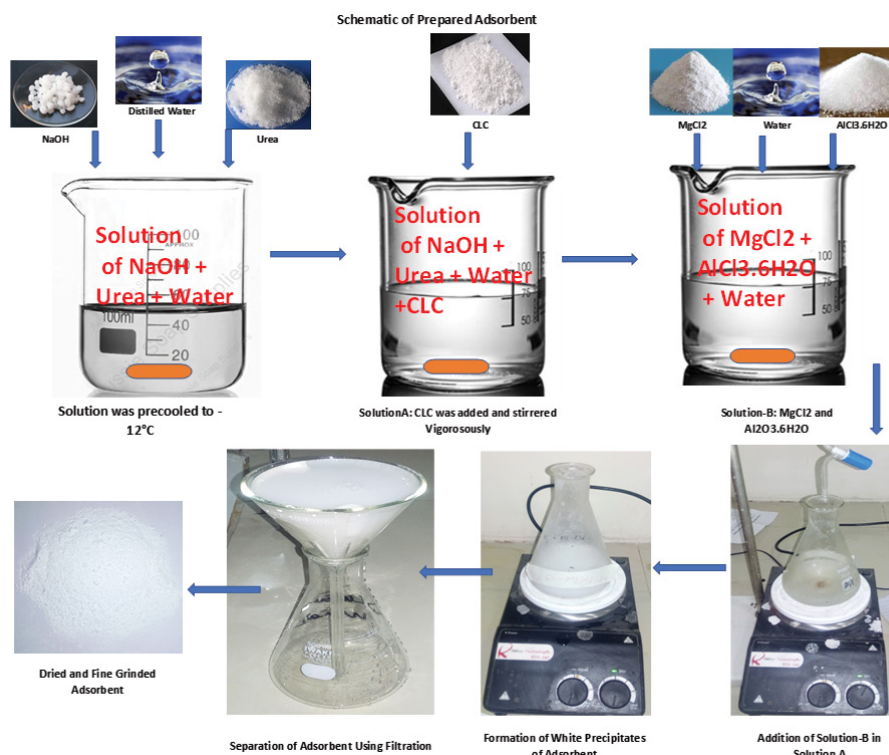


Fig. 1. Schematic diagram of adsorbent synthesis.

CLC using salt-ice bath [44]. Later, CLC was added under vigorous stirring. It resulted in a thick and clear solution confirming that CLC was completely dissolved. It is referred as solution A. Another solution having Mg<sup>2+</sup> and Al<sup>3+</sup> elemental molar ratios of 3:1 was prepared by adding 0.25 moles of AlCl<sub>3</sub>·6H<sub>2</sub>O and 0.75 moles of MgCl<sub>2</sub>·6H<sub>2</sub>O and in 50 mL deionized water. It is referred as solution B.

Solution A was filled in a 500 mL flask and adjusted on magnetic stirrer. Later solution B was added dropwise at 300 rpm by adjusting pH of solution A at 10. NaOH and HCl were used to adjust pH. Soon after addition of solution B in solution A, white colored precipitates were formed which were aged for 18 h at room temperature. Precipitates filtration was done with filter paper size of 0.2 μm and washed with 30% solution of ethyl alcohol in water. After washing all precipitates were kept in microwave oven (Thermaks) at 30°C for whole day and ground to fine powder using a ceramic pedestal.

### 2.3. Characterization of CLC and the adsorbent

The CLC and synthesized adsorbent were characterized using XRD (X-Ray Diffraction) PANalytical X-ray diffractometer, FTIR (Fourier transform infrared spectroscopy) using Bruker Vertex 70 model and BET (Brunauer-Emmett-Teller) using BET and BJP models. The adsorbent was also characterized using TEM (transmission electron microscopy) using Hitachi H-7600 model, SEM (Scanning electron microscopy) using Hitachi S-4800 scanning, AFM (atomic force microscopy) using Park Systems NX10 model, and zeta potential using pH drift method.

### 2.4. Adsorption studies

A 1,000 ppm solution of arsenic(III) was prepared as stock solution by adding calculated quantity of NaAsO<sub>2</sub> in 1 L deionized water. Different solutions of desired concentrations were prepared using this stock solution. All trials were conducted using 100 mL glass reactor having 50 mL of arsenic solution having concentration of 150 ppb. Flask was stirred magnetically at 150 rpm for varying experimental conditions of pH, adsorbent dose, temperature, and contact time. After stirring, solution, 0.2 μm PTFE membrane filters were used for filtration. Filtrate was examined for residual arsenic concentration on ICP-ES Shamarzoo-9000. Optimum values of pH, reaction time, temperature and initial adsorbent dose were investigated for maximum removal of arsenic. Initial pH adjustment was done using 0.1 M HCl and NaOH. The pH was examined in a range of 4–8. The adsorbent dose was varied from 0.13 to 1.33 g/L to determine the optimum dose. Isotherm and thermodynamic studies were also conducted. For these, initial concentration ranged from 100 to 1,500 ppb, temperature from 20°C to 40°C. For kinetic studies the reaction time was selected from 2 to 40 min.

## 3. Results and discussions

### 3.1. Characterization of CLC and the adsorbent

XRD plots of CLC and the adsorbent are given in Fig. 2a and b, respectively. The figures show that the peaks at different 2θ values for CLC were different than that of the peaks of the adsorbent. This comparison revealed that peaks

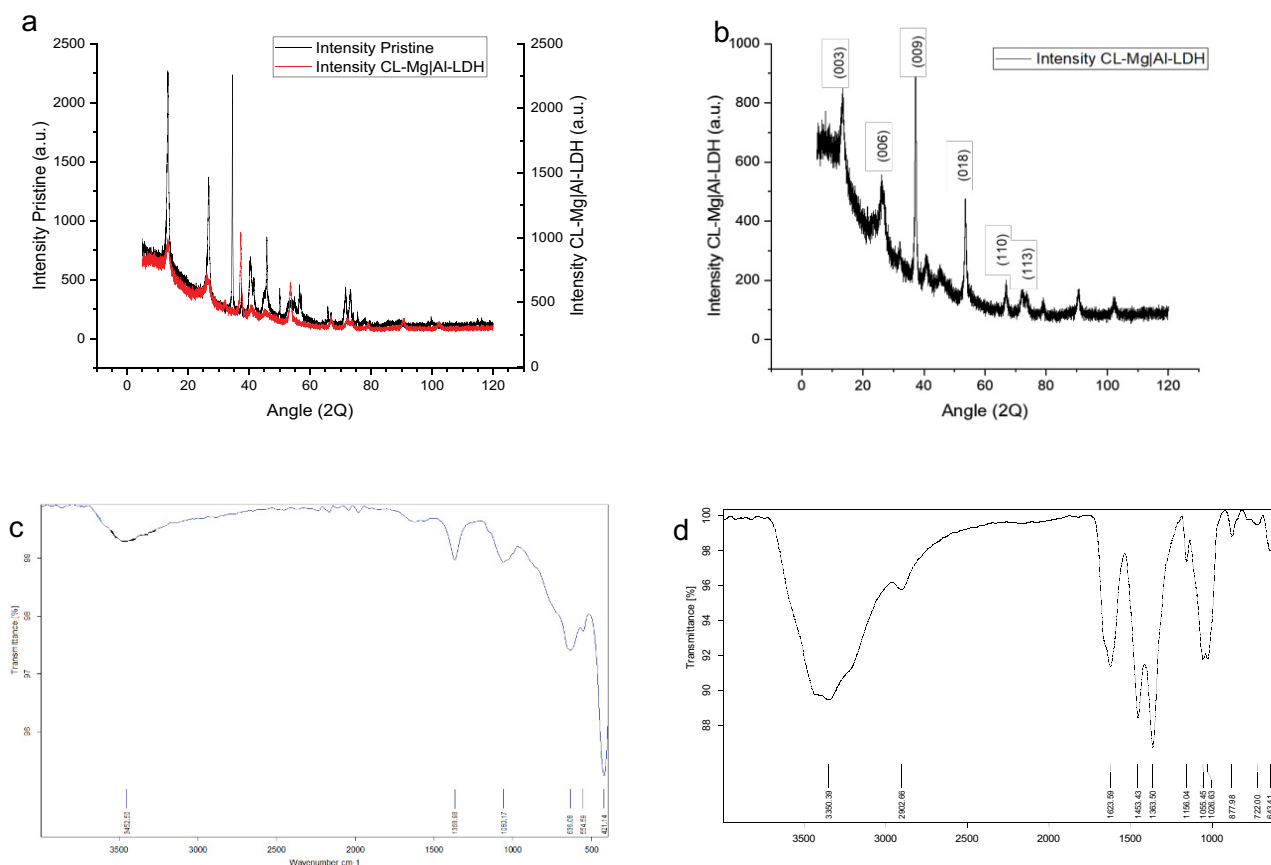


Fig. 2. Comparison of CLC and adsorbent XRD (a), XRD of adsorbent (b), FTIR of CLC (c) and FTIR of adsorbent (d).

at  $34.5^\circ$  and  $26.5^\circ$  had different intensities confirming successful modification of CLC surface with the attachment of metals. The presence of CLC was confirmed because of diffraction peaks at  $2\theta = 34.5^\circ$  [45]. Peaks representing planes (1 1 0), (0 0 6), (0 0 9) and (0 1 8) are assigned to Mg/Al LDH as shown in Fig. 2b. Peaks showing good dispersion of metal ions in layers of LDH corresponds to planes (0 1 8), (1 1 0) and (1 1 3) [45]. The sharpness and symmetry of peaks showed high crystalline phase LDH as confirmed from emergence of intense reflection peaks at  $13.37^\circ$ ,  $26.5^\circ$ ,  $34.5^\circ$  and  $40.5^\circ$  [17,35].

FTIR plot of CLC and adsorbent are given in Fig. 2c and d, respectively. Peaks in the ranges of 3,000–3,500, 1,000–1,500 and from 400 to 800 are identical in both the plots confirming presence of functional groups of CLC in adsorbent. Broad peak around 3,452.50 in Fig. 2c indicates OH<sup>-</sup> group. Fig. 2d shows that broad peak for OH<sup>-</sup> was shifted to 3,350.39 cm<sup>-1</sup> and small peak at 1,623.59 cm<sup>-1</sup>, which shows carboxylic group. CLC presence was indicated by small peak around 1,363.5 cm<sup>-1</sup> in both plots [46,47]. Tension and vibration of C–H bond in pyronose ring were due to emergence of medium peak at 2,902.66 cm<sup>-1</sup> while this peak was negligible in case of CLC indicating the influence of NaOH and urea solution. Presence of CLC was also confirmed from intense peak at 1,026.63 cm<sup>-1</sup>, weak peaks at 1,156.04 and 877.89 cm<sup>-1</sup> [48]. Glucosidic bonds C–O–C are confirmed from the presence of smallest peak at 1,156.04 cm<sup>-1</sup> [26].

M–O and O–M–O bonds where M can be Al or Mg<sup>2+</sup> were confirmed from emergence of peaks below 800 cm<sup>-1</sup> [45]. FTIR results confirmed the formation of required bonds in adsorbent. A clear difference of modification in CLC surface after application of Mg and Al metals can be seen from differences in peaks of both materials. Shift in peaks intensity and location confirmed successful synthesis of required adsorbent.

TEM results are shown in Fig. 3. It may be seen in Fig. 3a and b that size of nanoparticles ranged from 17 to 25.5 nm; it did not exceed 100 nm, hence confirming that particles were nano sized. The aggregation of particles was confirmed from AFM as shown in Fig. 3c and d. From both the TEM and AFM images sheet like structure of particles were confirmed. The peak height of the materials ranged from 10 to 50 nm which confirmed that material was nanocomposite [45]. Comparison of TEM images with similar studies showed that nanostructures were reinforced and evenly distributed in CLC medium [35]. Fig. 3e and f show SEM images of the adsorbent. In all magnified images rough and porous structure of the adsorbent could be observed. TEM and SEM showed similar results as that of XRD findings [35].

Fig. 4a shows spectrum of adsorbent obtained as a result of EDS analysis which showed presence of carbon (C), Mg, Al, oxygen (O), nitrogen (N) and chloride (Cl<sup>-</sup>). The elements were found to be in right composition resulting in the synthesis of the adsorbent. From the results, it can be predicted

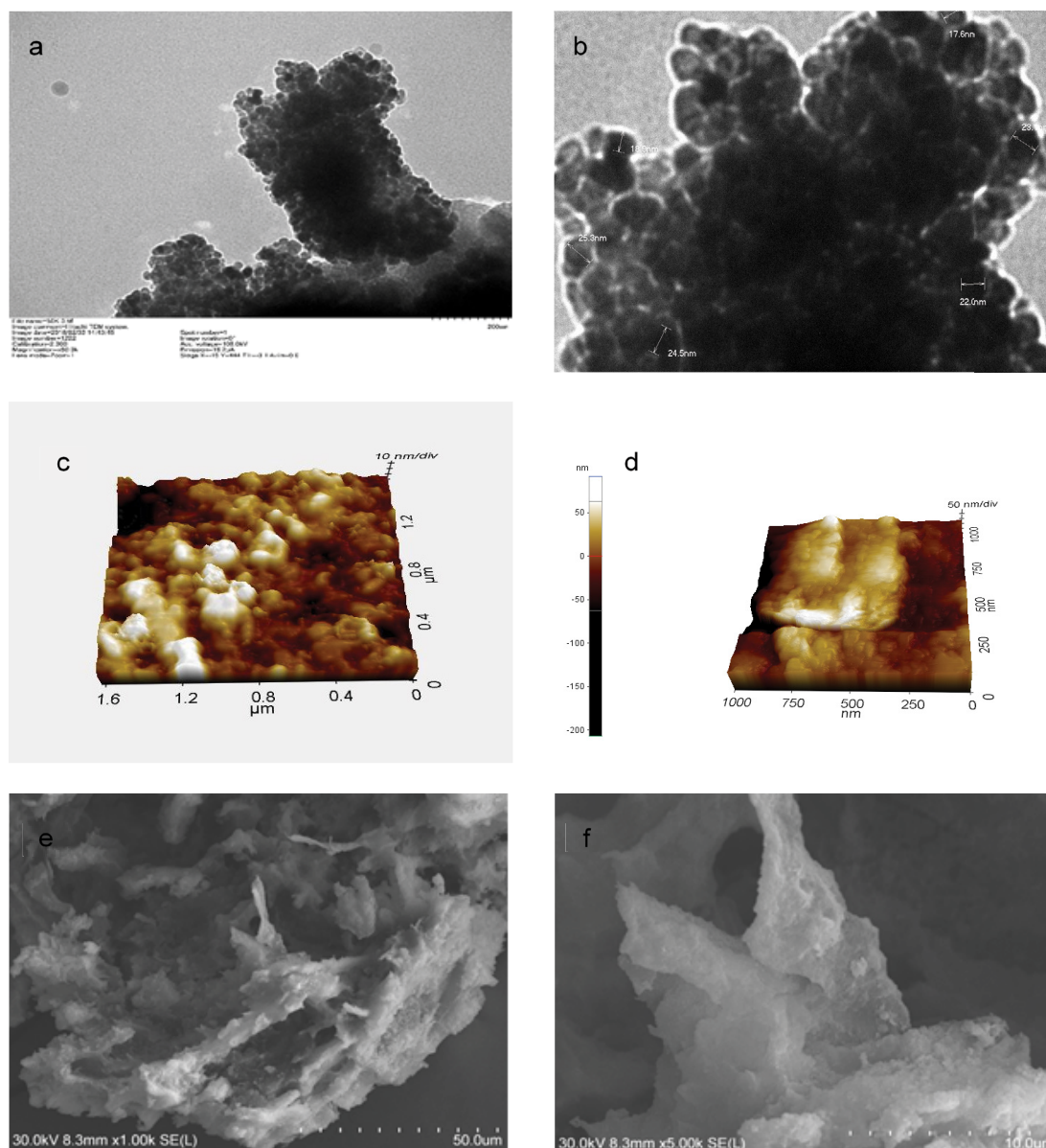


Fig. 3. TEM images (a and b), AFM Images (c and d) and SEM images (e and f) of adsorbent.

that urea, NaOH and CLC mixed solvent has major role in the synthesis of the adsorbent [35].

BET and BJH results showed that volume, size and surface area of pores and BJH desorption pore width of adsorbent were  $0.054 \text{ cm}^3/\text{g}$ ,  $126.0632 \text{ \AA}$ ,  $17.0684 \text{ m}^2/\text{g}$  and  $190.57 \text{ \AA}$  respectively. BET and BJH results for CLC showed that volume, size and surface area of pores and BJH desorption pore width were  $0.002377 \text{ cm}^3/\text{g}$ ,  $65.2054 \text{ \AA}$ ,  $1.4580 \text{ m}^2/\text{g}$  and  $100.326 \text{ \AA}$  respectively. Comparison of BET and BJH results for CLC and adsorbent showed that after application of Al and Mg metals on CLC in the presence of NaOH and urea, surface area and pore volume increased. It confirmed successful synthesis of adsorbent leading to more adsorption capacity.

BET and BJH results confirmed that adsorbent falls in the category of mesoporous materials. Surface area of

the adsorbent was greater than CL-Zn|Al LDH which was reported earlier [45]. From IUPAC classification of 1985, the current curve (Fig. 4b) resembled the Type-III with H3 hysteresis loop. Type-III isotherms confirmed that there is no identifiable monolayer formation present in adsorbent. It revealed weak adsorbent and adsorbate interactions [49].

The graph of initial pH of adsorbent and NaCl solution and its final pH is shown in Fig. 4c. The black line shows final pH after adsorbent addition while the red line shows initial pH. The point of zero charge  $\text{pH}_{\text{zpc}}$  of the adsorbent was found to be 8.4 which revealed that the adsorbent has surplus positive charge as compared to CLC material  $\text{pH}_{\text{zpc}} 6.0 \pm 0.05$  [50]. The change in the  $\text{pH}_{\text{zpc}}$  of adsorbent from CLC's  $\text{pH}_{\text{zpc}}$  indicated that CLC was modified during adsorbent preparation and loaded with Mg and Al metals. Hence, it confirmed that adsorbent was successfully synthesized.

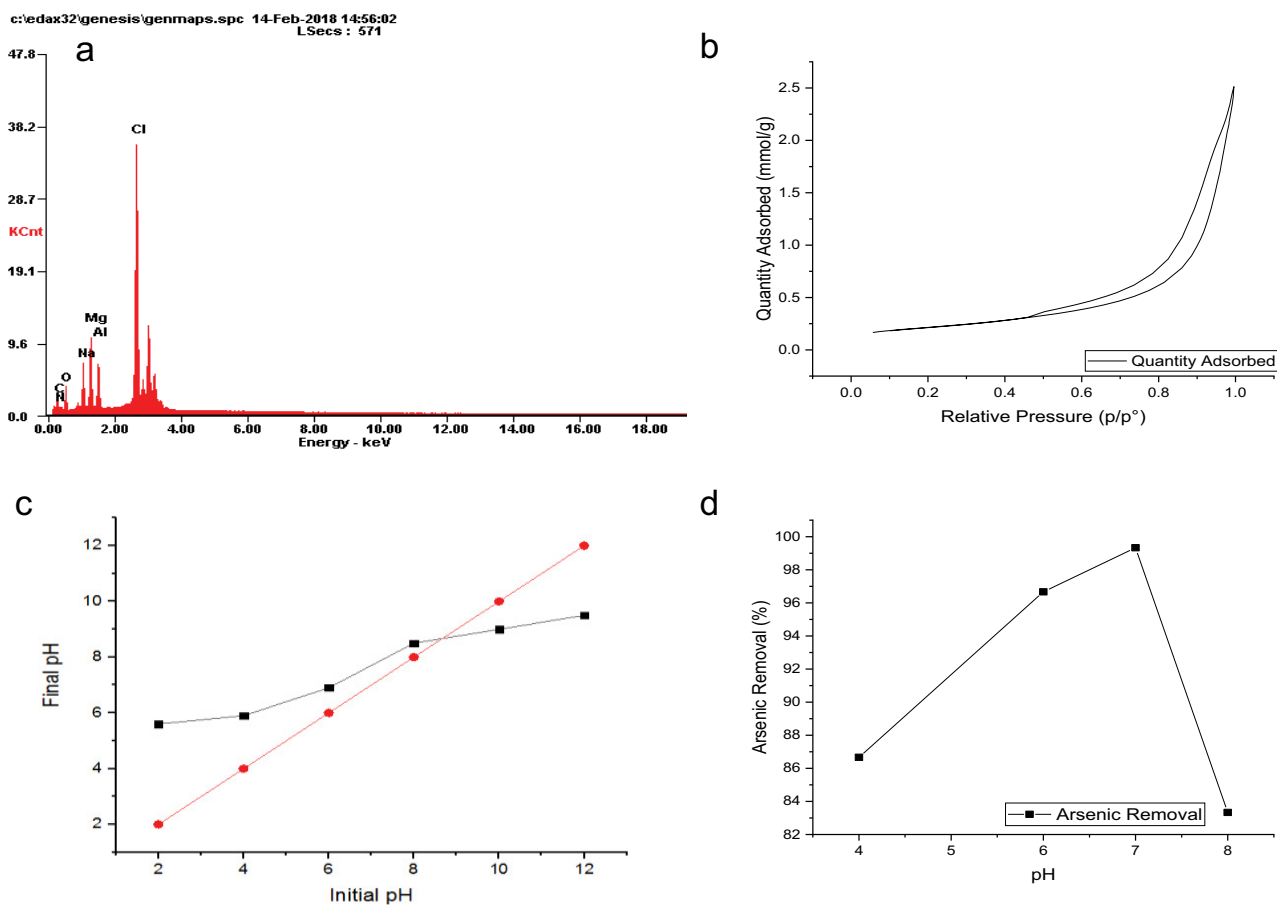


Fig. 4. EDS elemental graph (a), N<sub>2</sub> adsorption and desorption plot (b), plot of pH<sub>zpc</sub> (c) and pH optimization plot (d).

### 3.2. Optimization studies

#### 3.2.1. Initial pH effect on arsenic adsorption

Both the arsenic ions dissociation in water and the specification of active functional sites on adsorbent surface are pH dependent. Removal efficiency increased linearly from 86% to 99% when pH is raised from 4 to 7. After pH 7, the arsenic removal decreased (83%) as shown in Fig. 4d. At pH higher than 7, arsenic(III) starts adopting negative charge which hinders the adsorption of arsenic. It is because arsenic(III) has to compete with OH<sup>-</sup> ions for active sites [40,51].

At pH < 7, attachment of lone pair of electrons on functional group and H<sup>+</sup> compete with arsenic ions for adsorption sites, reducing arsenic removal [45,52]. The maximum adsorption of arsenic ions on adsorbent was observed at 7 pH.

#### 3.2.2. Dose effect on arsenic removal

From Fig. 5a it may be noted that arsenic removal had direct relationship with the adsorbent dose. The results show that the removal increased significantly with the dose. The removal reached approx. 98% at a dose of 0.67 g/L. Further increase in dose beyond 0.67 g/L did not significantly increase the arsenic removal. Hence, the optimum dose of adsorbent was concluded to be 0.67 g/L.

#### 3.2.3. Effect of reaction time

Fig. 5b shows faster arsenic uptake by adsorbent. Optimum contact time for arsenic removal was selected to be 25 min at which 99% arsenic removal was obtained.

#### 3.2.4. Effects of initial arsenic concentration

Arsenic uptake decreased with increasing initial concentration of arsenic as shown in Fig. 5c due to same number of active sites for a specific dose [45].

#### 3.2.5. Temperature optimization

With the increase in temperature the removal efficiency of arsenic increased slightly and 25°C was the optimum temperature as shown in Fig. 5d. Possible reasons for increase in removal with increase in temperature were swelling effect, expansion of atoms and increase in molecular vibrations leading more interaction between adsorbate and adsorbent [52,53].

### 3.3. Study of adsorption mechanism

#### 3.3.1. Adsorption kinetics

Adsorption kinetics and mechanism were evaluated using pseudo-first [Eq. (1)] and second-order [Eq. (2)] rate

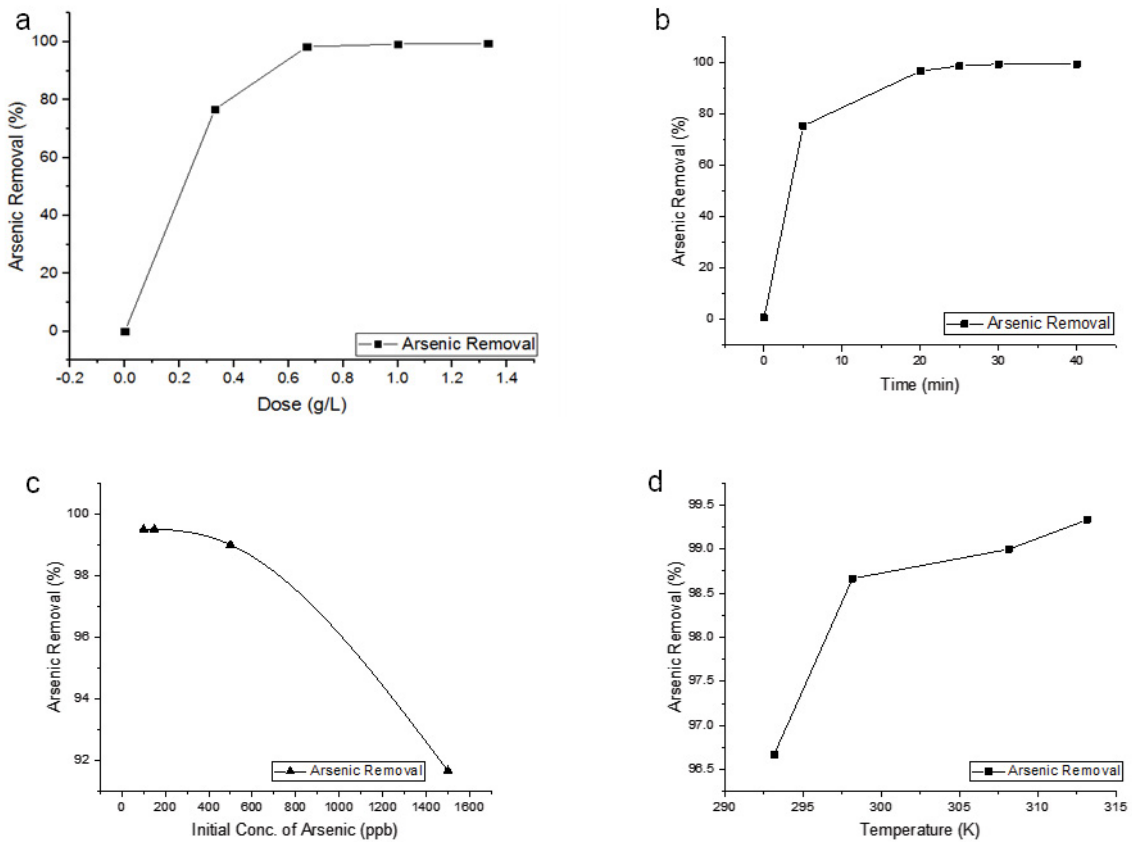


Fig. 5. Dose optimization (a) contact time (b), temperature optimization (c), and initial concentration (d).

equations in adsorption processes. Where  $q_t$  and  $q_e$  are adsorption capacities calculated at any time interval and at equilibrium respectively.  $K_1$  and  $K_2$  are rate constants for pseudo-first-order and pseudo-second-order reaction kinetics respectively. Units of  $K_1$  and  $K_2$  are (g/mg-min).

$$\log(q_e - q_t) = \log q_e + \frac{K_1}{2.303} \times t \quad (1)$$

$$\frac{t}{q_t} = \frac{1}{K_2 q_e^2} + \frac{1}{q_e} \times t \quad (2)$$

$R^2$  values and constants for all kinetic models are listed in Table 1. Arsenic removal using adsorbent fitted well for pseudo-second-order kinetic model having  $R^2$  value of 0.998 (Fig. 6b) while it was 0.927 for pseudo-first-order kinetics (Fig. 6a). It was revealed that adsorption of arsenic supports the assumptions of chemisorption process [54]. Previous studies conducted on LDHs showed similar correlation of data with second-order reaction kinetics [45,55].

The mechanism of the adsorption process was studied plotting the intraparticle diffusion model and Boyd model [Eqs. (3) and (4)] were used to differentiate film or intraparticle diffusion. Where  $q_t$  is adsorption capacity at time  $t$ ,  $k$ ,  $k_p$  and  $C$  are constants and  $q_e$  is adsorption capacity at equilibrium.

$$q_t = kt^{1/2} + C \quad (3)$$

$$\ln\left(1 - \frac{q_t}{q_e}\right) = k_p t \quad (4)$$

Linear fitting of data on intraparticle diffusion model predicts intraparticle diffusion while in case of deviation adsorption process might be controlled by two or three steps [56]. Intraparticle diffusion model plotted as shown in Fig. 6c clearly indicated that the process was controlled by two or three steps. First linear stage indicated the adsorption of arsenic ions on external surface of the adsorbent named as diffusion adsorption stage. Second linear stage assigned to intraparticle diffusion of arsenic ions through the pores of adsorbent. Final linear stage where slope becomes flat showed low rate of inter-particle diffusion because of less concentration of arsenic ions left in solution.

If linear form of Boyd model passes through origin, then intra-particle adsorption had occurred while opposite is considered as film diffusion. From Fig. 6d it can be seen that the linear plot of Boyd model did not pass through origin which indicated that film diffusion of arsenic particles on adsorbent surface had occurred.

### 3.3.2. Adsorption isotherms

The Langmuir, Freundlich and Temkin isotherms were used to find the mechanism of adsorption of arsenic on

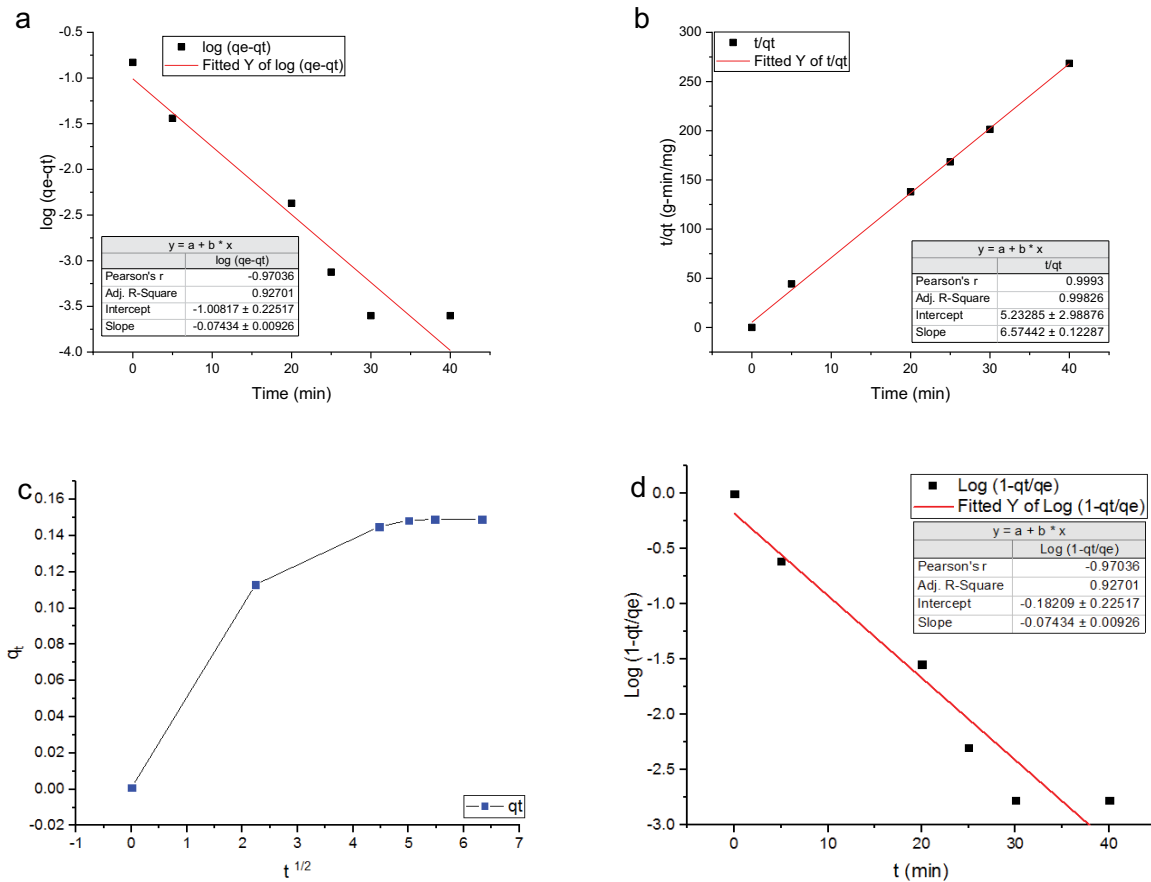


Fig. 6. Plot of pseudo-first-order (a), pseudo-second-order (b), intraparticle diffusion (c) and Boyd model (d).

the surface of the adsorbent. General and linear forms of Langmuir isotherm equation are shown in Eqs. (5) and (6).

$$q_e = q_m \frac{K_{ads} \times C_e}{1 + K_{ads} \times C_e} \tag{5}$$

$$\frac{1}{q_e} = \frac{1}{K_{ads} \times q_m} \frac{1}{C_e} + \frac{1}{q_m} \tag{6}$$

where  $q_e$  = adsorption capacity at equilibrium (mg/g),  $q_m$  = maximum adsorption capacity (mg/g),  $K_s$  = empirical Langmuir constant (L/mg),  $C_e$  = aqueous concentration of adsorbate (mg/L),  $q_m$  and  $K_{ads}$  obtained from linearized form as shown in Eq. (6). Separation factor is given in Eq. (7).

$$R_L = \frac{1}{1 + K_{ads} \times C_o} \tag{7}$$

where  $C_o$  is the initial concentration of the adsorbate and  $R_L$  is the separation factor. Freundlich and linearized Freundlich isotherm is given in Eqs. (8) and (9) respectively.

$$q_e = K_f C_e^{1/n} \tag{8}$$

$$\log q_e = \log K_f + \frac{1}{n} \log C_e \tag{9}$$

where  $k_f$  = Freundlich adsorption, that is, maximum adsorption capacity (mass of adsorbate/mass of the adsorbent when  $n = 1$ )  $1/n$  = Intensity of adsorption which gives value of affinity of adsorbent for adsorbate. Strength of attraction between adsorbent and adsorbate along with bond strength distribution on sites of adsorbent surface can be described with  $k_f$  and  $n$ .

Eqs. (10) and (11) are Temkin isotherm equations which assumes that heat of adsorption of all particles in a film

Table 1  
Kinetics parameters for arsenic adsorption of adsorbent

Pseudo-first-order				Pseudo-second-order			Intraparticle diffusion		Boyd model	
$q_{exp}$ (mg/g)	$q_e$ (mg/g)	$K_1$ (min <sup>-1</sup> )	$R^2$	$q_e$ (mg/g)	$K_2$ (g/mg min)	$R^2$	$K_i$ (mg/g min)	$R^2$	$K_b$	$R^2$
0.149	0.098	0.017	0.927	0.152	8.260	0.998	0.023	0.84	-0.0743	0.922

declines linearly with coverage of adsorbent surface with adsorbate ions.

$$q_e = B_T \ln A_T + B_T \ln C_e \tag{10}$$

$$B_T = \frac{RT}{b_T} \quad \& \quad A_T = \frac{R \times T}{b_T} \tag{11}$$

where  $R$  is real gas constant (8.314 J/Kmol),  $A_T$  as Temkin isotherm equilibrium binding constant (L/g),  $b_T$  is Temkin isotherm constant related to adsorption heat while  $B_T$  is also a constant for adsorption heat (J/mol) which shows adsorption as physical or chemical.

Langmuir, Freundlich and Temkin plots as shown in Fig. 7a–c, respectively. Parameters corresponding to relevant

isotherms are listed in Table 2. The results show that the data fitted better with Langmuir isotherm model with  $R^2$  value of 0.99. It shows the adsorbent followed monolayer adsorption process. The results obtained from isotherm studies highly supported the pseudo-second-order kinetics as described in previous section [45].

From Fig. 7a it is found that adsorption process also followed Freundlich isotherm which shows that there are multiple sites on adsorbent surface having different affinity for arsenic ions while each site followed Langmuir isotherm. It is evident from FTIR and  $\text{pH}_{zpc}$  studies that adsorbent surface is composed of different active sites including  $-\text{OH}$ ,  $-\text{O}-\text{Mg}-\text{OH}$ ,  $-\text{O}-\text{Al}-\text{OH}$  and neutral CLC surface. During adsorption process arsenic ions can be attached with all these sites at a time. Al and Mg metals formed anion exchange sites therefore, adsorption

Table 2  
Summary of isotherm parameters

Freundlich isotherm				Langmuir isotherm			Temkin		
$q_{\text{exp}}$ (mg/g)	$N$ (-)	$k_f$ (mg/g)	$R^2$	$q_m$ (mg/g)	$K_{\text{ads}}$ (g/mg min)	$R^2$	$A$ (L/g)	$B$ (J/mol)	$R^2$
1.375	2.15	0.168	0.939	1.460	8.260	0.999	0.023	0.84	0.982

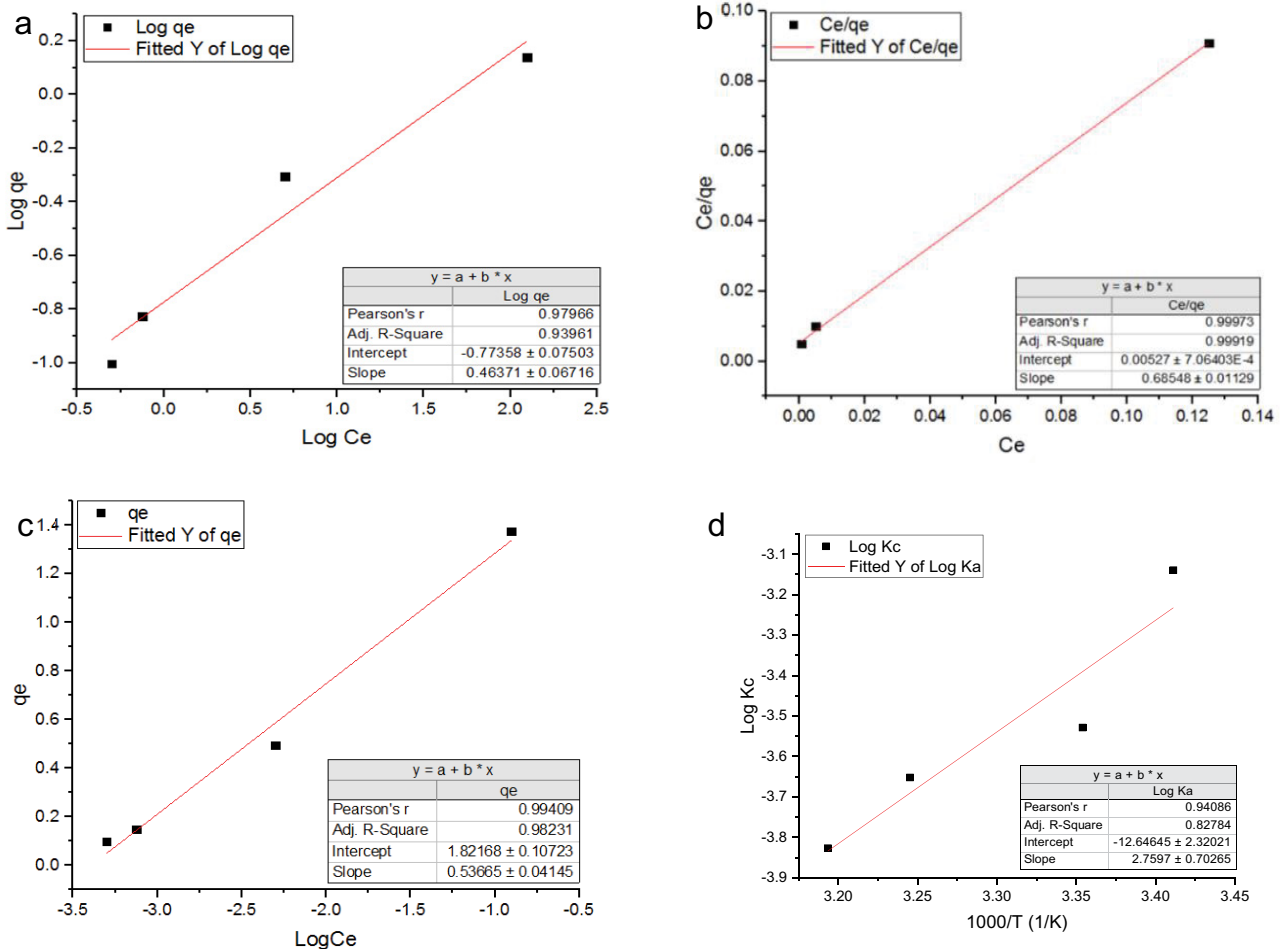


Fig. 7. Plot of Freundlich isotherm (a), Langmuir isotherm (b), Temkin isotherm (c) and Vant Hoff plot (d).

Table 3  
Maximum adsorption capacities of arsenic(III) on different adsorbents

Adsorbents	Adsorption capacity (mg/g)	References
Uncalcined chloride-LDHs	0.086	[57]
Iron oxide coated sand	0.136	[58]
Activated bauxsol	0.541	[59,60]
Activated alumina	0.18	[61]
Nano-scale zero valent Iron	2.47	[62]
Polymetallic sea nodule	0.69	[63]
Manganese ore	0.53	[64]
GAC	0.09	[65]
Olive pulp activated carbon	0.855	[66]
Pine wood char	0.0012	[67]
Oak wood char	0.006	
Oak bark char	0.0074	
CL-Mg Al-LDH	1.46	Current study

occurred on hydroxyl groups of both metals which acted as coagulation sites [45].

Adsorption process followed Temkin isotherm which showed that heat of adsorption decreased linearly with increase in layer of arsenic ions on adsorbent surface rather than logarithmic. It confirmed that adsorption process is exothermic in nature because value of Temkin constant B was 0.84 as shown in Table 2.

The adsorption capacity of the nanocomposite for arsenic uptake was 1.46 mg/g calculated using Langmuir isotherm. Data presented in Table 2 indicate different constants extracted from isotherm models best fit curves.

$R_L$  factor was 0.04 which shows that adsorption of arsenic removal using adsorbent was highly favorable. Adsorption is favorable if separation factor varies between zero and one and in case separation factor shows zero value then adsorption will be permanent [52].

Adsorption capacity of adsorbent under study was compared with other adsorbents for arsenic(III) removal as shown in Table 3.

### 3.3.3. Adsorption thermodynamics

Thermodynamic parameters include change in enthalpy ( $\Delta H^\circ$ ), Gibbs free energy change ( $\Delta G^\circ$ ) and entropy of reaction ( $\Delta S^\circ$ ). Gibbs free energy change  $\Delta G^\circ$  is fundamental criterion of spontaneity.  $\Delta G^\circ$ ,  $\Delta H^\circ$  and  $\Delta S^\circ$  are thermodynamic parameters and calculated using Van't Hoff equations expressed in Eqs. (11)–(13).

Table 4  
Thermodynamic coefficients for Van't Hoff plot

$\Delta H^\circ$	$\Delta S^\circ$	$\Delta G^\circ$ (kJ/mol)				Van't Hoff plot details
		293 K	298 K	308 K	313 K	
-52.84	-242.02	-18.071	-19.282	-21.702	-22.912	$R^2$

$$\Delta G^\circ = -RT \ln K_c \quad (12)$$

$$\Delta G^\circ = \Delta H^\circ - T\Delta S^\circ \quad (13)$$

$$K_a = \frac{q_i}{C_o} \quad (14)$$

where  $q_i$  = equilibrium adsorption capacity (mg/g),  $C_o$  = initial concentration (mg/L),  $R$  = universal gas constant (J/mol-K),  $T$  = absolute temperature (K) is calculated using  $K_c$  which is obtained from Langmuir model.

Fig. 7d is a plot of  $\log K_c$  against  $1/T$  known as Van't Hoff.  $\Delta H^\circ$  and  $\Delta S^\circ$  were obtained using slope and intercept of the plot respectively and  $\Delta G^\circ$  was calculated from these two values using Eq. (12). Table 4 shows data obtained from Van't Hoff plot. The value of  $\Delta H^\circ$  was -52.84 kJ/mol which confirmed that the adsorption process was exothermic which shows characteristics of chemisorption process.

Negative values of  $\Delta G^\circ$  confirmed that adsorption was spontaneous, that is, reaction will take place without any external assistance if started. Thermodynamic and Temkin isotherm studies revealed that reaction showed a shift towards exothermic nature. The possible reason was electrostatic force of attraction of arsenic ions towards active sites. Increase in negative values of  $\Delta G^\circ$  by increasing temperature, revealed that temperature and spontaneous nature were inversely related. Negative values of  $\Delta S^\circ$  showed decrease of randomness at the interface of adsorbent and solution during adsorption.

### 3.4. Leaching of metals from adsorbent surface to solution

Concentration of  $Al^{3+}$  in treated effluent was found to be 15.54 mg/L while  $Mg^{2+}$  concentration was 0.017 mg/L. Leaching of metal ions can be explained using hard and soft acids and bases (HSAB) concept known as Pearson acid base-base concept [68]. CLC acted as a weak base, Al as strong acid while  $Mg^{2+}$  forms a weak acid. Therefore,  $Mg^{2+}$  acting as weak acid tends to bind strongly with CLC, a weak base [69,70]. Same phenomenon was explained using variation of charge on metals surface with change in pH. At pH 7  $Al^{3+}$  had no charge on its surface which reduced forces of attraction between CLC surface and caused excessive leaching of  $Al^{3+}$  [71]. In contrary  $Mg^{2+}$  occurs in the form of  $Mg^{+2}$  at pH 7, therefore,  $Mg^{2+}$  has strong bonding and leaching was less [72].

### 3.5. CLC biodegradation

CLC was coated with bulk concentration of  $Mg^{2+}$  and Al metals which act as bacteriocyte. So, growth of bacteria

Table 5  
Comparison of cost for different groundwater arsenic removal techniques

Treatment method	Cost US\$/m <sup>3</sup>
Activated alumina used as adsorbent [75]	1.08
Reverse osmosis [75]	1.18
Cake alum and anionic polymeric flocculant [75]	0.76
CLC-Mg Al LDH	0.15
Activated carbon as adsorbent	0.07

on CLC surface will be slow until and unless concentration of metals on adsorbent surface is low [73].

### 3.6. Cost estimation of arsenic removal using adsorbent

Using 200 ppb arsenic concentration and adsorption capacity of 1.46 mg/g cost of arsenic removal was estimated to be US\$ 0.15/m<sup>3</sup>. Similar concentration was used previously to calculate cost [74]. Comparison of cost with other methods is shown in Table 5. Cost of adsorbent was less than that of reverse osmosis, activated alumina, alum and anionic polymeric flocculants.

### 3.7. Limitations in research work

This study has some limitations, that is, reuse, recycle and desorption studies were not conducted.

## 4. Conclusions and recommendations

The prepared adsorbent structure was crystalline, nanosized with particle diameter ranging from 17 to 25.5 nm, sheet like and well agglomerated with rough and porous surface. Surface area, size and volume of pores in the adsorbent were found to be 17.068 m<sup>2</sup>/g, 126.063 Å and 0.053 mm<sup>3</sup>/g. Surface area and volume of pores were greater than that of CLC indicating modification of CLC surface with metals in presence of urea and NaOH. Optimization studies revealed that adequate removal of arsenic was achieved at 25 min, at pH 7, dose of 0.667 g/L and 25°C. Isotherm results revealed that adsorption process followed Langmuir isotherm along with maximum adsorption capacity of 1.46 mg/g. Overall 99.3% removal at 150 ppb initial arsenic concentration was achieved with effluent concentration of 1 ppb. Kinetic data, isotherm and thermodynamic analysis showed that adsorption process was chemisorption, exothermic with spontaneous nature. Treatment cost was found to be 0.15 US\$/m<sup>3</sup> of water which was less than activated alumina (1.08 US\$/m<sup>3</sup>) and other materials previously used for arsenic removal.

It is recommended to

- Synthesize the same adsorbent using different Mg<sup>2+</sup> to Al<sup>3+</sup> ratios and conduct reuse and regeneration studies.
- Apply synthesized adsorbent on real ground water samples containing arsenic.
- Report the selectivity of the adsorbent towards arsenic removal.

- Study of recovery and reusability of the synthesized adsorbent along with its stability.

## Acknowledgement

Help of Sidra Iftekhar, Varsha Srivastava and Mika Sillanpää from Laboratory of Green Chemistry, School of Engineering Science, Lappeenranta University of Technology, Sammonkatu 12, FI-50130 Mikkeli, Finland for providing support in laboratory testing is acknowledged.

## Funding sources

This research did not receive any specific grant from funding agencies in the public, commercial, or not-for-profit sectors.

## References

- [1] U. Asghar, F. Perveen, S.K. Alvi, F.A. Khan, I. Siddqui, T.H. Usmani, Contamination of arsenic in public water supply schemes of Larkana and Mirpurkhas Districts of Sind, *J. Chem. Soc. Pak.*, 28 (2006) 130–135.
- [2] J.G. Hering, P.-Y. Chen, J.A. Wilkie, M. Elimelech, S. Liang, Arsenic removal by ferric chloride, *J. Am. Water Works Assn.*, 88 (1996) 155–167.
- [3] P. Askari, A. Faraji, G. Khayatian, S. Mohebbi, Effective ultrasound-assisted removal of heavy metal ions As(III), Hg(II), and Pb(II) from aqueous solution by new MgO/CuO and MgO/MnO<sub>2</sub> nanocomposites, *J. Iran Chem. Soc.*, 14 (2017) 613–621.
- [4] S. Zavareh, M. Zarei, F. Darvishi, H. Azizi, As(III) adsorption and antimicrobial properties of Cu-chitosan/alumina nanocomposite, *Chem. Eng. J.*, 273 (2015) 610–621.
- [5] C. Babu, B. Palanisamy, B. Sundaravel, K. Shanthi, V. Murugesan, Dihalogen crosslinked Fe<sub>3</sub>O<sub>4</sub>-reduced graphene oxide nanocomposites for arsenic and mercury adsorption, *Sci. Adv. Mater.*, 7 (2015) 794–805.
- [6] D. Chakraborti, M.M. Rahman, B. Das, A. Chatterjee, D. Das, B. Nayak, A. Pal, U.K. Chowdhury, S. Ahmed, B.K. Biswas, Groundwater arsenic contamination and its health effects in India, *Hydrogeol. J.*, 25 (2017) 1165–1181.
- [7] A. Azizullah, M.N.K. Khattak, P. Richter, D.-P. Häder, Water pollution in Pakistan and its impact on public health—a review, *Environ. Int.*, 37 (2011) 479–497.
- [8] M. Bibi, M.Z. Hashmi, R.N. Malik, Human exposure to arsenic in groundwater from Lahore district, Pakistan, *Environ. Toxicol. Pharmacol.*, 39 (2015) 42–52.
- [9] A.S. Qureshi, *Climate Change and Water Resources in South Asia*, AA Balkema Publishers, Leiden, 2005, pp. 197–230.
- [10] R. Nickson, J. McArthur, B. Shrestha, T. Kyaw-Myint, D. Lowry, Arsenic and other drinking water quality issues, Muzaffargarh District, Pakistan, *Appl. Geochem.*, 20 (2005) 55–68.
- [11] S. Muhammad, M.T. Shah, S. Khan, Arsenic health risk assessment in drinking water and source apportionment using multivariate statistical techniques in Kohistan region, northern Pakistan, *Food Chem. Toxicol.*, 48 (2010) 2855–2864.
- [12] M. Islam-Ul-Haq, N. Deedar, H. Wajid, Groundwater Arsenic Contamination—A Multi Directional Emerging Threat to Water Scarce Areas of Pakistan, 6th International IAHS Groundwater Quality Conference, Fremantle, Western Australia, 2007.
- [13] A.Z.M. Badruddoza, Z.B.Z. Shawon, W.J.D. Tay, K. Hidajat, M.S. Uddin, Fe<sub>3</sub>O<sub>4</sub> cyclodextrin polymer nanocomposites for selective heavy metals removal from industrial wastewater, *Carbohydr. Polym.*, 91 (2013) 322–332.
- [14] S. Sobhani, M. Bazrafshan, A.A. Delluei, Z.P. Parizi, Phospho-Michael addition of diethyl phosphite to  $\alpha$ ,  $\beta$ -unsaturated malonates catalyzed by nano  $\gamma$ -Fe<sub>2</sub>O<sub>3</sub>-pyridine based catalyst as a new magnetically recyclable heterogeneous organic base, *Appl. Catal., A*, 454 (2013) 145–151.

- [15] A. Farooqi, H. Masuda, N. Firdous, Toxic fluoride and arsenic contaminated groundwater in the Lahore and Kasur districts, Punjab, Pakistan and possible contaminant sources, *Environ. Pollut.*, 145 (2007) 839–849.
- [16] S. Iftekhhar, M.U. Farooq, M. Sillanpää, M.B. Asif, R. Habib, Removal of Ni(II) using multi-walled carbon nanotubes electrodes: relation between operating parameters and capacitive deionization performance, *Arabian J. Sci. Eng.*, 42 (2017) 235–240.
- [17] S. Iftekhhar, V. Srivastava, M. Sillanpää, Enrichment of lanthanides in aqueous system by cellulose based silica nanocomposite, *Chem. Eng. J.*, 320 (2017) 151–159.
- [18] R.J. Gohari, W. Jye Lau, T. Matsuura, A.F. Ismail, Remediation of Heavy Metals in the Environment, CRC Press, Boca Raton, Florida, USA, 2016, pp. 413–438.
- [19] P. Brandhuber, G. Amy, Alternative methods for membrane filtration of arsenic from drinking water, *Desalination*, 117(1998) 1–10.
- [20] A.A. Alswat, M.B. Ahmad, T.A. Saleh, Zeolite modified with copper oxide and iron oxide for lead and arsenic adsorption from aqueous solutions, *J. Water Supply Res. Technol. AQUA*, 65 (2016) 465–479.
- [21] M. Yang, T.-J. Jiang, Z. Guo, J.-H. Liu, Y.-F. Sun, X. Chen, X.-J. Huang, Sensitivity and selectivity sensing cadmium(II) using amination functionalized porous SnO<sub>2</sub> nanowire bundles-room temperature ionic liquid nanocomposite: combined efficient cation capture with control experimental conditions, *Sens. Actuators, B*, 240 (2017) 887–894.
- [22] S. Carfagna, N. Lanza, G. Salbitani, A. Basile, S. Sorbo, V. Vona, Physiological and morphological responses of Lead or Cadmium exposed *Chlorella sorokiniana* 211–8K (Chlorophyceae), *SpringerPlus*, 2 (2013) 147, doi: 10.1186/2193-1801-2-147.
- [23] D. Mohan, C.U. Pittman Jr., Arsenic removal from water/wastewater using adsorbents—a critical review, *J. Hazard. Mater.*, 142 (2007) 1–53.
- [24] S. Zhou, D. Wang, H. Sun, J. Chen, S. Wu, P. Na, Synthesis, characterization, and adsorptive properties of magnetic cellulose nanocomposites for arsenic removal, *Water Air Soil Pollut.*, 225 (2014) 1945.
- [25] M. Fanadzo, D. Zireva, E. Dube, A. Mashingaidze, Evaluation of various substrates and supplements for biological efficiency of *Pleurotus sajor-caju* and *Pleurotus ostreatus*, *Afr. J. Biotechnol.*, 9 (2010) 2756–2761.
- [26] H. Zhu, Y. Jia, X. Wu, H. Wang, Removal of arsenic from water by supported nano zero-valent iron on activated carbon, *J. Hazard. Mater.*, 172 (2009) 1591–1596.
- [27] C. Kamala, K. Chu, N. Chary, P. Pandey, S. Ramesh, A. Sastry, K.C. Sekhar, Removal of arsenic(III) from aqueous solutions using fresh and immobilized plant biomass, *Water Res.*, 39 (2005) 2815–2826.
- [28] A.A. Alswata, M.B. Ahmad, N.M. Al-Hada, H.M. Kamari, M.Z.B. Hussein, N.A. Ibrahim, Preparation of zeolite/zinc oxide nanocomposites for toxic metals removal from water, *Results Phys.*, 7 (2017) 723–731.
- [29] R. Attinti, D. Sarkar, K. Barrett, R. Datta, Adsorption of arsenic(V) from aqueous solutions by goethite/silica nanocomposite, *Int. J. Environ. Sci. Technol.*, 12 (2015) 3905–3914.
- [30] C.-H. Liu, Y.-H. Chuang, T.-Y. Chen, Y. Tian, H. Li, M.-K. Wang, W. Zhang, Mechanism of arsenic adsorption on magnetite nanoparticles from water: thermodynamic and spectroscopic studies, *Environ. Sci. Technol.*, 49 (2015) 7726–7734.
- [31] J.A. Gomes, P. Daida, M. Kesmez, M. Weir, H. Moreno, J.R. Parga, G. Irwin, H. McWhinney, T. Grady, E. Peterson, Arsenic removal by electrocoagulation using combined Al-Fe electrode system and characterization of products, *J. Hazard. Mater.*, 139 (2007) 220–231.
- [32] T. Sun, Z. Zhao, Z. Liang, J. Liu, W. Shi, F. Cui, Efficient As(III) removal by magnetic CuO-Fe<sub>3</sub>O<sub>4</sub> nanoparticles through photo-oxidation and adsorption under light irradiation, *J. Colloid Interface Sci.*, 495 (2017) 168–177.
- [33] B. Chen, Z. Zhu, J. Ma, M. Yang, J. Hong, X. Hu, Y. Qiu, J. Chen, One-pot, solid-phase synthesis of magnetic multiwalled carbon nanotube/iron oxide composites and their application in arsenic removal, *J. Colloid Interface Sci.*, 434 (2014) 9–17.
- [34] J. Tuček, R. Prucek, J. Kolář, G. Zoppellaro, M. Petr, J. Filip, V.K. Sharma, R. Zbořil, Zero-valent iron nanoparticles reduce arsenites and arsenates to As(0) firmly embedded in core-shell superstructure: challenging strategy of arsenic treatment under anoxic conditions, *ACS Sustainable Chem. Eng.*, 5 (2017) 3027–3038.
- [35] N. Ponomarev, Synthesis of Novel Cellulose Based Nanocomposites by Green Methods and Their Possible use as Adsorbents, School of Engineering Science Laboratory of Green Chemistry, Lappeenranta University of Technology, Finland, 2017.
- [36] M. Auffan, J. Rose, O. Proux, D. Borschneck, A. Masion, P. Chaurand, J.-L. Hazemann, C. Chaneac, J.-P. Jolivet, M.R. Wiesner, Enhanced adsorption of arsenic onto maghemite nanoparticles: As(III) as a probe of the surface structure and heterogeneity, *Langmuir*, 24 (2008) 3215–3222.
- [37] I. Andjelkovic, D.N. Tran, S. Kabiri, S. Azari, M. Markovic, D. Losic, Graphene aerogels decorated with  $\alpha$ -FeOOH nanoparticles for efficient adsorption of arsenic from contaminated waters, *ACS Appl. Mater. Interfaces*, 7 (2015) 9758–9766.
- [38] H. Li, C. Shan, Y. Zhang, J. Cai, W. Zhang, B. Pan, Arsenate adsorption by hydrous ferric oxide nanoparticles embedded in cross-linked anion exchanger: effect of the host pore structure, *ACS Appl. Mater. Interfaces*, 8 (2016) 3012–3020.
- [39] K. Grover, S. Komarneni, H. Katsuki, Uptake of arsenite by synthetic layered double hydroxides, *Water Res.*, 43 (2009) 3884–3890.
- [40] E. Otgonjargal, Y.-S. Kim, S.-M. Park, K. Baek, J.-S. Yang, Mn-Fe layered double hydroxides for adsorption of As(III) and As(V), *Sep. Sci. Technol.*, 47 (2012) 2192–2198.
- [41] Q. Wang, Q. Lin, Q. Li, K. Li, L. Wu, S. Li, H. Liu, As(III) removal from wastewater and direct stabilization by in-situ formation of Zn-Fe layered double hydroxides, *J. Hazard. Mater.*, 403 (2021) 123920, doi: 10.1016/j.jhazmat.2020.123920.
- [42] A. Abo Markeb, A. Alonso, A.D. Dorado, A. Sánchez, X. Font, Phosphate removal and recovery from water using nanocomposite of immobilized magnetite nanoparticles on cationic polymer, *Environ. Technol.*, 37 (2016) 2099–2112.
- [43] S. Ahmad, Water Resources Development and Management in Pakistan, The Pakistan Development Review Part II (Winter 2007), pp. 911–937.
- [44] J. Cai, L. Zhang, Rapid dissolution of cellulose in LiOH/urea and NaOH/urea aqueous solutions, *Macromol. Biosci.*, 5 (2005) 539–548.
- [45] S. Iftekhhar, V. Srivastava, M. Sillanpää, Synthesis and application of LDH intercalated cellulose nanocomposite for separation of rare earth elements (REEs), *Chem. Eng. J.*, 309 (2017) 130–139.
- [46] S.-M. Li, N. Jia, J.-F. Zhu, M.-G. Ma, R.-C. Sun, Synthesis of cellulose-calcium silicate nanocomposites in ethanol/water mixed solvents and their characterization, *Carbohydr. Polym.*, 80 (2010) 270–275.
- [47] M.-G. Ma, F. Deng, K. Yao, Manganese-containing cellulose nanocomposites: the restrain effect of cellulose treated with NaOH/urea aqueous solutions, *Carbohydr. Polym.*, 111 (2014) 230–235.
- [48] R. Buchanan, H. Caspers, J. Murphy, Lattice vibration spectra of Mg(OH)<sub>2</sub> and Ca(OH)<sub>2</sub>, *Appl. Opt.*, 2 (1963) 1147–1150.
- [49] M. Thommes, K. Kaneko, A.V. Neimark, J.P. Olivier, F. Rodriguez-Reinoso, J. Rouquerol, K.S. Sing, Physisorption of gases, with special reference to the evaluation of surface area and pore size distribution (IUPAC Technical Report), *Pure Appl. Chem.*, 87 (2015) 1051–1069.
- [50] I.A. Udoetok, R.M. Dimmick, L.D. Wilson, J.V. Headley, Adsorption properties of cross-linked cellulose-epichlorohydrin polymers in aqueous solution, *Carbohydr. Polym.*, 136 (2016) 329–340.
- [51] M. Lim, G.-C. Han, J.-W. Ahn, K.-S. You, H.-S. Kim, Leachability of arsenic and heavy metals from mine tailings of abandoned metal mines, *Int. J. Environ. Res. Public Health*, 6 (2009) 2865–2879.

- [52] G. Vijayakumar, R. Tamilarasan, M. Dharmendirakumar, Adsorption, kinetic, equilibrium and thermodynamic studies on the removal of basic dye Rhodamine-B from aqueous solution by the use of natural adsorbent perlite, *J. Mater. Environ. Sci.*, 3 (2012) 157–170.
- [53] S. Muryanto, S.D. Hadi, Adsorption laboratory experiment for undergraduate chemical engineering: introducing kinetic, equilibrium and thermodynamic concepts, *IOP Conf. Ser.: Mater. Sci. Eng.*, 162 (2016) 012004, doi: 10.1088/1757-899X/162/1/012004.
- [54] Y.-S. Ho, Review of second-order models for adsorption systems, *J. Hazard. Mater.*, 136 (2006) 681–689.
- [55] C. Qing, Study on the adsorption of lanthanum(III) from aqueous solution by bamboo charcoal, *J. Rare Earths*, 28 (2010) 125–131.
- [56] Q. Yuan, N. Li, Y. Chi, W. Geng, W. Yan, Y. Zhao, X. Li, B. Dong, Effect of large pore size of multifunctional mesoporous microsphere on removal of heavy metal ions, *J. Hazard. Mater.*, 254 (2013) 157–165.
- [57] G.P. Gillman, A simple technology for arsenic removal from drinking water using hydrotalcite, *Sci. Total Environ.*, 366 (2006) 926–931.
- [58] O.S. Thirunavukkarasu, T. Viraraghavan, K.S. Subramanian, O. Chaalal, M.R. Islam, Arsenic removal in drinking water—impacts and novel removal technologies, *Energy Sources*, 27 (2005) 209–219.
- [59] H. Genç-Fuhrman, J.C. Tjell, D. McConchie, Increasing the arsenate adsorption capacity of neutralized red mud (Bauxsol), *J. Colloid Interface Sci.*, 271 (2004) 313–320.
- [60] H. Genç-Fuhrman, J.C. Tjell, D. McConchie, Adsorption of arsenic from water using activated neutralized red mud, *Environ. Sci. Technol.*, 38 (2004) 2428–2434.
- [61] T.S. Singh, K.K. Pant, Equilibrium, kinetics and thermodynamic studies for adsorption of As(III) on activated alumina, *Sep. Purif. Technol.*, 36 (2004) 139–147.
- [62] S.R. Kanel, B. Manning, L. Charlet, H. Choi, Removal of arsenic(III) from groundwater by nanoscale zero-valent iron, *Environ. Sci. Technol.*, 39 (2005) 1291–1298.
- [63] S. Maity, S. Chakravarty, S. Bhattacharjee, B. Roy, A study on arsenic adsorption on polymetallic sea nodule in aqueous medium, *J. Water Res.*, 39 (2005) 2579–2590.
- [64] S. Chakravarty, V. Dureja, G. Bhattacharyya, S. Maity, S. Bhattacharjee, Removal of arsenic from groundwater using low cost ferruginous manganese ore, *J. Water Res.*, 36 (2002) 625–632.
- [65] B.E. Reed, R. Vaughan, L. Jiang, As(III), As(V), Hg, and Pb removal by Fe-oxide impregnated activated carbon, *J. Environ. Eng.*, 126 (2000) 869–873.
- [66] T. Budinova, N. Petrov, M. Razvigorova, J. Parra, P. Galiatsatou, Removal of arsenic(III) from aqueous solution by activated carbons prepared from solvent extracted olive pulp and olive stones, *Ind. Eng. Chem. Res.*, 45 (2006) 1896–1901.
- [67] D. Mohan, C.U. Pittman Jr., M. Bricka, F. Smith, B. Yancey, J. Mohammad, P.H. Steele, M.F. Alexandre-Franco, V. Gómez-Serrano, H. Gong, Sorption of arsenic, cadmium, and lead by chars produced from fast pyrolysis of wood and bark during bio-oil production, *J. Colloid Interface Sci.*, 310 (2007) 57–73.
- [68] P.W. Ayers, The physical basis of the hard/soft acid/base principle, *Faraday Discuss.*, 135 (2007) 161–190.
- [69] R.G. Pearson, Hard and soft acids and bases, *J. Am. Chem. Soc.*, 85 (1963) 3533–3539.
- [70] R.F. Nalewajski, Electrostatic effects in interactions between hard (soft) acids and bases, *J. Am. Chem. Soc.*, 106 (1984) 944–945.
- [71] E. Matijević, L.J. Stryker, Coagulation and reversal of charge of lyophobic colloids by hydrolyzed metal ions: III. Aluminum sulfate, *J. Colloid Interface Sci.*, 22 (1966) 68–77.
- [72] L. Semerjian, G. Ayoub, High-pH-magnesium coagulation–flocculation in wastewater treatment, *Adv. Environ. Res.*, 7 (2003) 389–403.
- [73] P. Morgan, T.H. Frost, Germicide, United States Patent Office, Official Gazzete 1942.
- [74] C.C. Mólgora, A.M. Domínguez, E.M. Avila, P. Drogui, G. Buelna, Removal of arsenic from drinking water: a comparative study between electrocoagulation-microfiltration and chemical coagulation-microfiltration processes, *Sep. Purif. Technol.*, 118 (2013) 645–651.
- [75] M. Piñón-Miramontes, R.G. Bautista-Margulis, A.J.F. Pérez-Hernández, Removal of arsenic and fluoride from drinking water with cake alum and a polymeric anionic flocculent, *Fluoride*, 36 (2003) 122–128.